Inverse Problems **25** (2009) 045007 (16pp) doi:10.1088/0266-5611/25/4/045007

An improved fixed-point algorithm for determining a Tikhonov regularization parameter

Fermín S Viloche Bazán[1] **and Juliano B Francisco**

Department of Mathematics, Federal University of Santa Catarina, Florianópolis SC, Santa Catarina CEP 88040-900, Brazil

E-mail: fermin@mtm.ufsc.br and juliano@mtm.ufsc.br

Received 5 September 2008, in final form 19 January 2009
Published 17 February 2009
Online at stacks.iop.org/IP/25/045007

Abstract

We re-analyze a Tikhonov parameter choice rule devised by Regińska (1996 *SIAM J. Sci. Comput.* **3** 740–49) and algorithmically realized through a fast fixed-point (FP) method by Bazán (2008 *Inverse Problems* **24** 035001). The method determines a Tikhonov parameter associated with a point near the L-corner of the maximum curvature and at which the L-curve is locally convex. In practice, it works well when the L-curve presents an L-shaped form with distinctive vertical and horizontal parts, but failures may occur when there are several local convex corners. We derive a simple and computable condition which describes the regions where the L-curve is concave/convex, while providing insight into the choice of the regularization parameter through the L-curve method or FP. Based on this, we introduce variants of the FP algorithm capable of handling the parameter choice problem even in the case where the L-curve has several local corners. The theory is illustrated both graphically and numerically, and the performance of the variants on a difficult ill-posed problem is evaluated by comparing the results with those provided by the L-curve method, generalized cross-validation and the discrepancy principle.

(Some figures in this article are in colour only in the electronic version)

1. Introduction

Least square problems arising from ill-posed problems (also called discrete ill-posed problems),

$$\min_{f\in\mathbb{R}^n} \|Af - g\|_2, \qquad A \in \mathbb{R}^{m\times n}(m \geqslant n), \quad g \in \mathbb{R}^m, \tag{1.1}$$

need to be regularized. The main difficulty in these problems is that small errors in the data can be enormously magnified in the solution, because the coefficient matrix is severely

[1] This research was sponsored by CNPq, Brasil, grant 473481/08-1.

ill-conditioned. Perhaps the earliest and most well-known method to deal with this class of problems is due to Tikhonov [18]. The underlying idea of Tikhonov's method is to replace (1.1) by the minimization problem

$$f_\lambda = \arg\min_{f\in\mathbb{R}^n} \left\{ \|Af - g\|_2^2 + \lambda^2 \|Lf\|_2^2 \right\}, \tag{1.2}$$

where L is chosen to incorporate desirable properties on the solution such as smoothness, and λ is a positive parameter called the regularization parameter. The problem is how to choose the parameter λ such that f_λ becomes as close as possible to the noisy-free solution.

Parameter-choice strategies are commonly divided into two classes: *a priori* strategies and *a posteriori* strategies. The difference between these is that while *a priori* strategies try to select the regularization parameter before doing numerical computations, *a posteriori* strategies try to select the regularization parameter from the results (e.g., f_λ) and the given right-hand side. This last class covers the discrepancy principle (DP) of Morozov [14], the L-curve criterion of Hansen and O'Leary [8], generalized cross-validation (GCV) of Heath, Golub and Wabba [3] and a fixed-point method (FP method) recently introduced by Bazán [1], among others; for a survey on Tikhonov parameter choice rules see [9] and references therein. More recent references can be found in [2, 5, 6, 11–13, 16, 19]. Attributes and properties of parameter choice rules are well documented in a number of papers and we do not elaborate about this any further here; instead we will concentrate on certain features of the FP method which motivated this work. For simplicity of exposition, the L-curve criterion will be denoted by LC and the FP method by FP. FP can be regarded as a realization of a parameter choice rule devised by Regińska [15], who proposed as the regularization parameter a local minimum of the function

$$\Psi_\mu(\lambda) = x(\lambda) y^\mu(\lambda), \tag{1.3}$$

for proper $\mu > 0$, where $y(\lambda) = \|f_\lambda\|_2^2$ (or $y(\lambda) = \|Lf_\lambda\|_2^2$) and $x(\lambda) = \|g - Af_\lambda\|_2^2$. Bazán investigated the properties of $\Psi_\mu(\lambda)$ and concluded that its minimizers are converging values of a sequence defined by

$$\lambda_{k+1} = \phi_\mu(\lambda_k), \qquad k \geqslant 0, \tag{1.4}$$

where

$$\phi_\mu(\lambda) = \sqrt{\mu}\frac{\|g - Af_\lambda\|_2}{\|f_\lambda\|_2}, \qquad \lambda > 0. \tag{1.5}$$

Having defined the quantities above, we can briefly describe FP by saying that it starts with a proper initial guess and then proceeds with the iterates (1.4) until a minimizer of Ψ_μ is captured. There are two remarkable characteristics of FP to be mentioned here. First, FP converges very quickly since only a few solution (semi)norms and corresponding residual norms are required (see the numerical results reported in [1]), and second, FP is closely related to LC: for every L-curve displaying an L-shaped form with distinctive vertical and horizontal parts, there corresponds a function ϕ_μ having a unique fixed-point at which the L-curve is locally convex, the fixed-point being associated with a point near the L-corner of the maximum curvature. These characteristics justify the performance of FP when compared to LC and other methods, as reported in [1].

Unfortunately, FP is not always without difficulties and our experience with it in cases where the L-curve displays several convex corners has been unsatisfactory, due mainly to the fact that the suggested starting value sometimes leads to regularization parameters which yield undersmoothed solutions (this will be illustrated in the following section). The purpose of the present paper is to introduce variants of the FP algorithm designed in order to overcome the difficulties mentioned above.

This paper is structured as follows. As FP depends on fixed-points at which the L-curve is locally convex, the convexity properties of such curve are analyzed in section 2. Our main result is expressed in terms of a simple and readily computable/verifiable condition, which determines the regions in which the L-curve is concave/convex, thereby providing insight into the decision on how to select the regularization parameter when using parameter choice rules such as FP or LC. From the theoretical point of view, this result not only complements earlier convexity analyses performed independently by Regińska [15] and Hansen [7], but also provides insight into the convexity properties of the L-curve on the whole domain. The use of fixed-points in determining convexity regions of the L-curve is also exploited. The variants of FP to be proposed are described in section 3. In section 4, the performance of one of the proposed variants on a difficult discrete ill-posed problem is evaluated and compared with results provided by DP, LC and GCV.

We end the section with some preliminary results and notation used throughout this paper. As usual, we assume that L is $p \times n$, $\operatorname{rank}(L) = p \leqslant n$, and that the pair (A, L) have a GSVD

$$A = U \begin{bmatrix} \Sigma & 0 \\ 0 & I_{n-p} \end{bmatrix} X, \qquad L = V[M; 0]X. \tag{1.6}$$

Here both $U = [u_1, \ldots, u_n] \in \mathbb{R}^{m\times n}$ and $V = [v_1, \ldots, v_p] \in \mathbb{R}^{p\times p}$ have orthonormal columns, $X \in \mathbb{R}^{n\times n}$ is nonsingular and Σ, M are diagonal matrices: $\Sigma = \operatorname{diag}(\sigma_1, \ldots, \sigma_p)$, $M = \operatorname{diag}(\mu_1, \ldots, \mu_p)$. Define $\alpha_i = \left|u_i^T g\right|^2$ (the squared Fourier coefficient of g), $\delta_0 = \|(I - UU^T)g\|_2$ (the size of the incompatible component of g that lies outside the column space of A). Let the generalized singular values of the pair (A, L), $\gamma_i = \sigma_i/\mu_i$ be arranged in nondecreasing order. Then it is easy to see that

$$x(\lambda) = \sum_{i=1}^{p} \frac{\lambda^4 \alpha_i}{\left(\gamma_i^2 + \lambda^2\right)^2} + \delta_0^2, \qquad y(\lambda) = \sum_{i=1}^{p} \frac{\gamma_i^2 \alpha_i}{\left(\gamma_i^2 + \lambda^2\right)^2} \tag{1.7}$$

and that for $\lambda > 0$ the derivatives with respect to λ of these functions satisfy

$$x'(\lambda) = 4\lambda^3 \sum_{i=1}^{p} \frac{\gamma_i^2 \alpha_i}{\left(\gamma_i^2 + \lambda^2\right)^3} > 0, \qquad y'(\lambda) = -4\lambda \sum_{i=1}^{p} \frac{\gamma_i^2 \alpha_i}{\left(\gamma_i^2 + \lambda^2\right)^3} < 0. \tag{1.8}$$

In addition, inequalities (1.7) and (1.8) lead to

$$\mathrm{d}y/\mathrm{d}x = -1/\lambda^2 \tag{1.9}$$

showing that y is a monotonically decreasing function of x. Finally, based on (1.7)–(1.8), straightforward computations lead to

$$\phi'_\mu(\lambda) > 0, \qquad \text{for} \quad \lambda > 0, \tag{1.10}$$

which show that ϕ_μ is a strictly increasing function. We close this section with the observation that throughout this paper no assumption is made on $\operatorname{rank}(A)$, but to ensure a unique solution to (1.2) we shall assume that $\operatorname{rank}([A^T L^T]^T) = n$.

2. On convexity of the L-curve

In view of the existing relationship between FP and LC, a complete description of the convexity properties of the L-curve is required in order to understand when and why these methods break down. A first step toward this was done by Regińska [15], who proved that if $\delta_0 = 0$ then the L-curve is concave on $(0, \gamma_1) \cup (\gamma_p, \infty)$, whereas if $\delta_0 \neq 0$, the L-curve is concave on (γ_p, ∞) and convex on $(0, \epsilon)$ with ϵ small enough. Regińska's analysis however does not extend to the interval $[\gamma_1, \gamma_p]$. Another analysis concerning the issue appears in a paper by

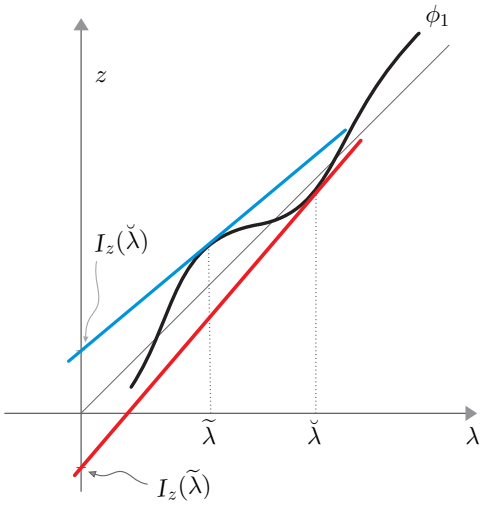

Figure 1. Geometric interpretation of condition (2.1).

Hansen [7]; there, concavity properties of the L-curve for $\gamma_1 \leqslant \lambda \leqslant \gamma_p$ are discussed but no definite conclusion is provided. As far as we know, there are no advances about this, and a precise description of the convexity properties of the L-curve is still lacking. In this section such a description is provided.

We start with a theorem showing that there is a close relationship between the convexity of the L-curve in a log–log scale and the behavior of the iteration function $\phi_1(\lambda)$.

Theorem 1. *Let $v = \log(y(\lambda))$, $u = \log(x(\lambda))$ and let $m_L(\lambda)$ denote the slope of the L-curve in a log–log scale at the point (u, v). Then the L-curve is convex in the vicinity of $\breve{\lambda}$ if and only if for all λ in the vicinity holds*

$$\phi_1'(\lambda) \leqslant \frac{\phi_1(\lambda)}{\lambda}. \tag{2.1}$$

Further, if (2.1) is strictly satisfied at $\lambda = \breve{\lambda}$, then the L-curve is locally strictly convex at $\breve{\lambda}$.

Proof. Differentiation with respect to λ shows that

$$\frac{\mathrm{d}v}{\mathrm{d}u} \doteq m_L(\lambda) = -\frac{(\phi_1(\lambda))^2}{\lambda^2}.$$

Taking derivative with respect to λ on both sides of this equation it follows that

$$\begin{aligned}\frac{\mathrm{d}^2 v}{\mathrm{d}u^2}\frac{x'(\lambda)}{x(\lambda)} &= m_L'(\lambda)\\ &= -2\frac{\phi_1(\lambda)}{\lambda}\left[\frac{\lambda\phi_1'(\lambda) - \phi_1(\lambda)}{\lambda^2}\right].\end{aligned}$$

Since $x'(\lambda)/x(\lambda)$ is always positive by (1.8), it follows that the L-curve is convex in the vicinity of $(u(\breve{\lambda}), v(\breve{\lambda}))$ if and only if the condition (2.1) holds in that vicinity, as claimed. The last assertion of the theorem is also immediate from (2.1). □

Condition (2.1) has a simple and nice geometric interpretation (see figure 1). To describe this let $T_{\breve{\lambda}}(\lambda)$ denote the tangent line to the curve $z = \phi_1(\lambda)$ at $(\breve{\lambda}, \phi_1(\breve{\lambda}))$, and let $(0, I_z(\breve{\lambda}))$ be the

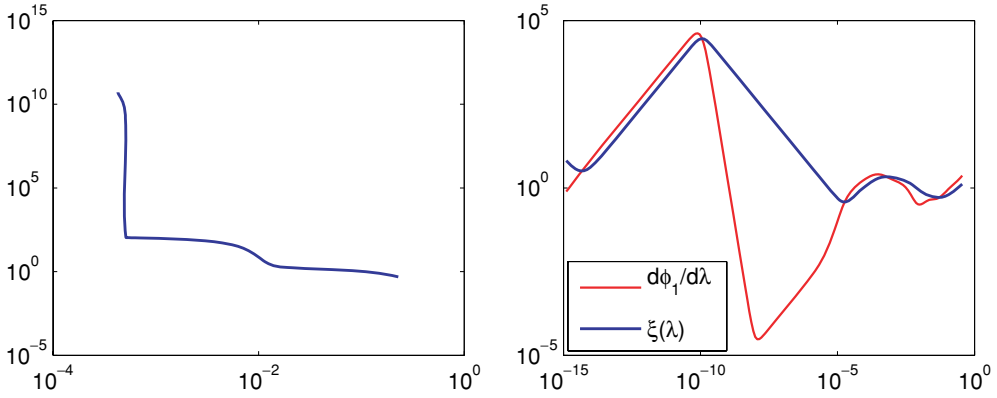

Figure 2. Left: L-curve of the test problem heat of size 64. Right: curves $z = \xi(\lambda)$ and $z = \phi_1'(\lambda)$ for $\gamma_1 \leqslant \lambda \leqslant \gamma_p$. Both curves are on a log–log scale.

intersection point of this line with the ordinate axis. Then since

$$T_{\check{\lambda}}(\lambda) = \{(\lambda, z), z = \phi_1(\check{\lambda}) + \phi_1'(\check{\lambda})(\lambda - \check{\lambda}), \lambda \geqslant 0\},$$

and $I_z(\check{\lambda}) = \phi_1(\check{\lambda}) - \check{\lambda}\phi_1'(\check{\lambda})$, it follows that the L-curve is strictly convex (resp. concave) in the vicinity of $\check{\lambda}$ if $T_{\check{\lambda}}(\lambda)$ intersects the ordinate axis above (resp. below) the origin, and that if the L-curve changes concavity at $\check{\lambda}$, then the tangent line crosses the origin.

A consequence of theorem 1 is that the critical points of the function $\xi(\lambda) = \phi_1(\lambda)/\lambda$, $\lambda > 0$, determine the regions in which the L-curve is convex/concave. More precisely, we shall prove that for every two consecutive zeros of the equation

$$\xi'(\lambda) = 0 \quad \Leftrightarrow \quad \phi_1'(\lambda) - \frac{\phi_1(\lambda)}{\lambda} = 0,$$

there is a region in which the L-curve is concave or convex depending on whether the sign of $\phi_1'(\lambda) - \frac{\phi_1(\lambda)}{\lambda}$ is either positive or negative in that region. For illustration purposes, the L-curve of a test problem from the regularization tools [10], as well as the associated function $\xi(\lambda)$ and $\phi_1'(\lambda)$ are depicted in figure 2. Note that the regions where the L-curve is convex (concave) agrees well with the regions where the curve $z = \phi_1'(\lambda)$ lies below (above) the curve $z = \xi(\lambda)$.

A mathematical description of what we have just demonstrated graphically can be described as follows:

Corollary 1. *Assume that the function $\xi(\lambda)$ attains two local extremes at two consecutive critical points of ξ, namely λ_1 and λ_2 with $\lambda_1 < \lambda_2$. Then the L-curve is convex on the interval (λ_1, λ_2) if λ_1 is a local maximum point, and the L-curve is concave on (λ_1, λ_2) if λ_1 is a local minimum point.*

Proof. Let us assume that ξ has a local maximum at λ_1 so that ξ is locally minimized at λ_2. Then based on the fact that ξ is continuous and differentiable for $\lambda > 0$, it follows that ξ is a nonincreasing function on $[\lambda_1, \lambda_2]$ and therefore

$$\xi'(\lambda) = \frac{\lambda\phi_1'(\lambda) - \phi_1(\lambda)}{\lambda^2} \leqslant 0, \qquad \text{for} \qquad \lambda_1 < \lambda < \lambda_2.$$

This inequality is equivalent to (2.1) and proves the first part of the corollary. The assertion concerning the concavity of the L-curve is proved similarly. □

Remark 1. When ϕ_1 has no fixed-point, which means $\phi_1(\lambda) > \lambda$ for $\lambda > 0$, a decision has to be taken concerning the choice of a parameter μ to ensure that the function ϕ_μ has a fixed-point that minimizes Ψ_μ. The FP algorithm, as originally described in [1], handles this heuristically (i.e., without theoretical support), looking for an approximate minimum of ξ which is then used to select a parameter μ. The choice of μ in this way is now theoretically supported by corollary 1.

Remark 2. Corollary 1 continues to hold if the assumption on λ_2 is replaced by a weaker one, where λ_2 is required to be a critical point instead of a local extremum. That is, corollary 1 holds regardless of whether λ_2 is an extremum point or not.

The next theorem shows that the fixed-points of $\phi_1(\lambda)$, when they exist, provide information that can be used to determine approximately the regions where the L-curve is concave/convex.

Theorem 2. *Assume λ^* is a fixed-point of $\phi_1(\lambda)$ satisfying $\phi_1''(\lambda^*) \neq 0$. Then the L-curve is convex in the vicinity of λ^* if and only if $-\lambda^* \frac{y'(\lambda^*)}{y(\lambda^*)} < 1$. Moreover, whenever this inequality holds, we have $\lambda^* < \frac{\sqrt{3}}{3}\gamma_p$, and there exists $\lambda_* \in (\lambda^*, \gamma_p)$ that is a fixed-point of ϕ_1 at which the L-curve is locally concave.*

Proof. Differentiation with respect to λ on both sides of the identity $(\phi_1(\lambda))^2 = \frac{x(\lambda)}{y(\lambda)}$ leads to

$$\begin{aligned} 2\phi_1(\lambda)\phi_1'(\lambda) &= \frac{y(\lambda)x'(\lambda) - x(\lambda)y'(\lambda)}{(y(\lambda))^2} \\ &= -\frac{\lambda^2 y(\lambda) + x(\lambda)}{(y(\lambda))^2} y'(\lambda), \end{aligned} \tag{2.2}$$

where we have used the fact that $x'(\lambda) = -\lambda^2 y'(\lambda)$ by (1.9), and hence

$$\phi_1'(\lambda^*) = -\frac{\lambda^{*2} + \phi_1(\lambda^*)^2}{2\phi_1(\lambda^*)} \frac{y'(\lambda^*)}{y(\lambda^*)} = -\frac{\lambda^* y'(\lambda^*)}{y(\lambda^*)}. \tag{2.3}$$

Assume

$$\phi_1'(\lambda^*) = -\frac{\lambda^* y'(\lambda^*)}{y(\lambda^*)} < 1.$$

Then, by continuity arguments it follows that there exists a vicinity of λ^* such that $\phi_1'(\lambda) < \phi_1(\lambda)/\lambda$ for all λ in the vicinity, and theorem 1 ensures that the L-curve is convex in this vicinity.

Conversely, if the L-curve is convex in the vicinity of λ^*, by theorem 1 we have that

$$-\frac{\lambda^* y'(\lambda^*)}{y(\lambda^*)} \leqslant 1, \tag{2.4}$$

and we have to prove equality is not possible in the above inequality. In fact, if $\phi_1'(\lambda^*) = 1$, then λ^* is a critical point of ξ and, since $\lambda^*\xi''(\lambda^*) = \phi_1''(\lambda^*)$, which is immediate to see, and since $\phi''(\lambda^*) \neq 0$ by hypothesis, it follows that λ^* is an extremum point of ξ, and consequently, by corollary 1, a point where the L-curve changes concavity, which is a contradiction. Thus we must have $\phi_1'(\lambda^*) = \lambda^* y'(\lambda^*)/y(\lambda^*) < 1$, as claimed.

To prove that $\lambda^* < \frac{\sqrt{3}}{3}\gamma_p$ observe that, similarly to the convex case, a necessary and sufficient condition for the L-curve to be locally concave at λ_* is $\phi_1'(\lambda_*) > 1$. With this observation in mind, assume now the statement to be proved is not true, i.e., assume that $\lambda^* \geqslant \frac{\sqrt{3}}{3}\gamma_p$. Then, due to (1.7)–(1.8) and the fact that the generalized singular values decay to zero without particular gap in the context of discrete ill-posed problems, which means there

holds $\gamma_i < \gamma_p$, for at least one $1 \leqslant i < p$, we have

$$-\lambda^* y'(\lambda^*) - y(\lambda^*) = \sum_{i=1}^{p} \frac{\left(3\lambda^{*2} - \gamma_i^2\right)\gamma_i^2 \alpha_i}{\left(\gamma_i^2 + \lambda^{*2}\right)^3} > 0 \quad \Rightarrow \quad -\frac{\lambda^* y'(\lambda^*)}{y(\lambda^*)} > 1,$$

thus implying that the L-curve is locally concave at λ^*, a contradiction. Therefore, $\lambda^{*2} < \gamma_p^2/3$.

To prove the last part we recall two results from [1]: (a) the fixed-points of ϕ_1, when they exist, belong to the interval $(0, \gamma_p)$, and (b) for all $\lambda > \gamma_p$ there holds $\phi_1(\lambda) \geqslant \lambda$. Thus, since local convexity of the L-curve at λ^* implies that $\phi_1(\lambda) < \lambda$ at least for some λ to the right of λ^*, it follows that the function $\lambda - \phi_1(\lambda)$ changes sign in the interval $(\lambda^*, \gamma_p]$ and hence, there is λ_* inside this interval such that $\phi_1(\lambda_*) = \lambda_*$. To complete the proof it is sufficient to see that the condition $\phi_1'(\lambda) > 1$ is satisfied in the vicinity sufficiently small of λ_*, which ensures the last assertion of the theorem. □

2.1. *On the condition* $\phi_1'(\lambda^*) < 1$ *and the assumption* $\phi_1''(\lambda^*) \neq 0$

If λ^* is a fixed-point of ϕ_μ, i.e., a point for which $\lambda^* = \sqrt{\mu}\phi_1(\lambda^*)$, let us analyze the role that both the condition $\phi_1'(\lambda^*) \leqslant 1$ and the assumption $\phi_1''(\lambda^*) \neq 0$ play in the minimization of the Regińska's functional Ψ_μ, and in the convexity of the L-curve. For this, we start by noting that the first and second order derivative of Ψ_μ at λ^* satisfy

$$\Psi_\mu'(\lambda^*) = \left[-\lambda^{*2} + \mu\phi_1^2(\lambda^*)\right] y^\mu(\lambda^*) y'(\lambda^*) = 0, \tag{2.5}$$

$$\Psi_\mu''(\lambda^*) = -2\lambda^*[1 - \sqrt{\mu}\phi_1'(\lambda^*)] y^\mu(\lambda^*) y'(\lambda^*), \tag{2.6}$$

where we have always $y^\mu(\lambda^*)y'(\lambda^*) < 0$ because of (1.8). Then, an immediate consequence of (2.6) (which supports the FP algorithm) is that Ψ_μ is always minimized as far as $\sqrt{\mu}\phi_1'(\lambda^*) < 1$, this is happening when $\phi_1'(\lambda^*) < 1$ and $\mu \leqslant 1$ or when $\phi_1'(\lambda^*) \leqslant 1$ and $\mu < 1$. However, (2.6) provides no information when $\phi_1'(\lambda^*) = 1/\sqrt{\mu}$ (since in this case $\Psi_\mu''(\lambda^*) = 0$), and in order to obtain informative results we have to analyze higher order derivatives of Ψ_μ. Restricting to third and fourth order derivatives, taking $\phi_1'(\lambda^*) = 1/\sqrt{\mu}$ we have

$$\Psi_\mu'''(\lambda^*) = 2\sqrt{\mu}\lambda^*\phi_1''(\lambda^*) y^\mu(\lambda^*) y'(\lambda^*), \tag{2.7}$$

and

$$\begin{aligned}\Psi_\mu''''(\lambda^*) = {} & 2\sqrt{\mu}[\lambda^*\phi_1'''(\lambda^*) + 3\phi_1''(\lambda^*)] y^\mu(\lambda^*) y'(\lambda^*) \\ & + 6\sqrt{\mu}\lambda^*\phi_1''(\lambda^*)[\mu y^{\mu-1}(\lambda^*) y'^2(\lambda^*) + y^\mu(\lambda^*) y''(\lambda^*)],\end{aligned} \tag{2.8}$$

where, as before, $y^\mu(\lambda^*)y'(\lambda^*) < 0$ is always valid.

Several conclusions can be derived from (2.7)–(2.8) provided some information about $\phi_1''(\lambda^*)$ is available. Some of these follow:

(1) If $\phi_1''(\lambda^*) \neq 0$, λ^* is an inflection point of Ψ_μ (see (2.7)).
(2) If $\phi_1''(\lambda^*) > 0$ and $\mu = 1$, λ^* is a local minimum point of ξ. This is because λ^* is also a critical point of ξ and because we noted that $\xi''(\lambda^*)$ and $\phi_1''(\lambda^*)$ share the same sign. As in this case the straight line $z = \lambda$ is tangent to the curve $z = \phi_1(\lambda)$ at $(\lambda^*, \phi_1(\lambda^*))$, which implies $\phi_1(\lambda) \geqslant \lambda \,\forall\, \lambda$ in some interval I containing λ^*, from this we can conclude that the L-curve changes from convex to concave inside I (see corollary 1). A similar conclusion can be drawn if $\phi_1''(\lambda^*) < 0$.
(3) When $\phi_1''(\lambda^*) = 0$, no information is available from (2.7) but reliable information can be extracted from (2.8) provided that $\phi_1'''(\lambda^*) \neq 0$. Of course, if $\phi_1''(\lambda^*) = 0$ and $\phi_1'''(\lambda^*) < 0$, for instance, then λ^* is a local minimum point of Ψ_μ.

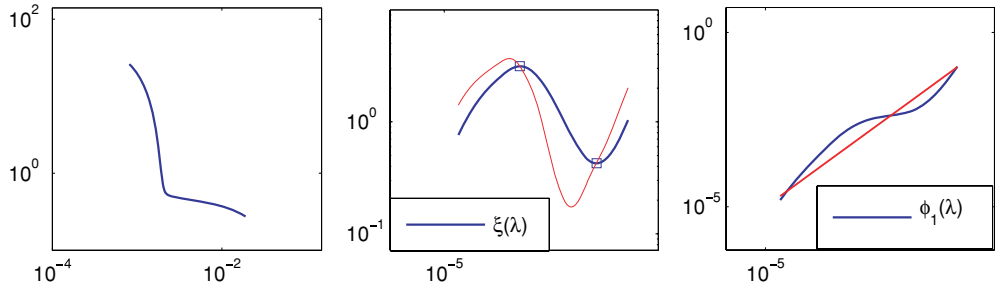

Figure 3. L-curve (left), concavity/convexity regions as determined by two local extremes of the function ξ (center), and curve $z = \phi_1(\lambda)$ (right) corresponding to the test problem deriv2 from regularization tools [10]. The straight line $z = \lambda$ is also included to illustrate that function ϕ_1 has three fixed-points. Small squares denote the points at which the L-curve changes concavity. All curves are on a log–log scale.

2.2. *Conclusions on convexity/concavity of the L-curve*

The theory described above is now used to obtain some conclusions. In the following, the largest fixed-point of ϕ_1, if any, is always denoted by λ_*. Also, for ease of comprehension, when $\delta_0 = 0$ and ξ has a local extremum, we shall assume the simplifying hypothesis that ξ has no more than one local extremum neither between consecutive fixed-points of ϕ_1 nor inside the interval (λ_*, γ_p). When $\delta_0 \neq 0$ and there exists a fixed-point λ^* that minimizes Ψ_1, we assume that ξ is not allowed to have more than two local extremes on the interval $(0, \lambda^*)$. The cases $\delta_0 = 0$ and $\delta_0 \neq 0$ are described separately

(i) The case $\delta_0 = 0$ is easy to analyze via our fixed-point approach. Of course, since ϕ_1 is always guaranteed to have at least one nonzero fixed-point on (γ_1, γ_n), see theorem 1 in [1], some conclusions can be drawn knowing the number of fixed-points of ϕ_1. For instance, if λ_* is the unique fixed-point of ϕ_1, then the L-curve will be concave on the whole domain provided ξ has no extremum point inside (γ_1, λ_*). If, on the other hand, we assume ϕ_1 has a unique fixed-point at which the L-curve is locally convex (i.e., Ψ_1 has a unique minimizer), which means ϕ_1 has three fixed-points (see theorem 1 in [1] again), the conclusion is that the L-curve changes concavity at least three times. More precisely, the L-curve will be concave between the origin and the local maximum of ξ, convex between the two local extremes of ξ, and concave to the right of the local minimum of ξ. This configuration is shown to hold when analyzing the test problem deriv2 from the regularization tools [10] (see figure 3).

(ii) If $\delta_0 \neq 0$, fixed-points of ϕ_1 are not always guaranteed to exist and the intervals of concavity/convexity of the L-curve may not be determined using fixed-point information. So, the definite answer about the question will ultimately depend on the number of local extremum of ξ. However, taking advantage of the fact that ξ has always a local minimum near the origin (guaranteed by Regińska's analysis) some conclusions can be now obtained. For instance, if ξ has a local maximum at λ_1, besides the local minimum near the origin, there will exist λ_2 (located to the right of λ_1) at which ξ has another local minimum, and if ξ has no extra local extremum, the conclusion is that the L-curve is convex on the interval $(0, \epsilon)$ (for small ϵ), concave on $(\epsilon, \lambda_1) \cup (\lambda_2, \infty)$ and convex on (λ_1, λ_2). The case where ξ has two local maxima and three local minima, as seen in figure 2, appears very often in problems where the function ϕ_1 has four fixed-points and the L-curve has two corners, one of the corners being associated with a very small λ. The conclusions for the case where ξ has more than two local maxima are straightforward.

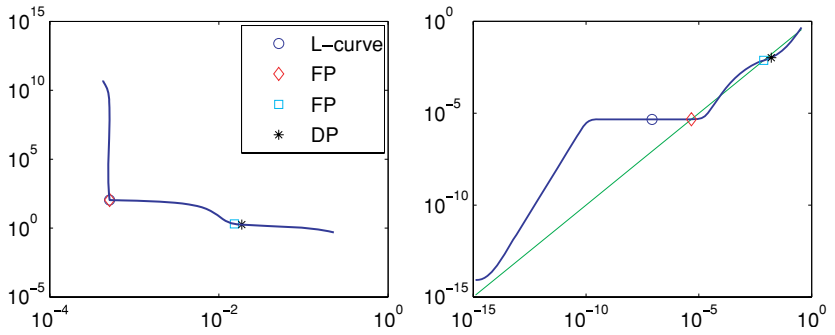

Figure 4. L-curve, curve $z = \phi_1(\lambda)$ with ϕ_1 having several fixed-points, and points corresponding to several Tikhonov parameters. The graphs correspond to the test problem heat.

Table 1. Numerical results for the test problem heat generated by the function *heat.m* with $\kappa = 1$, an exact solution norm $\|f^{\text{exact}}\|_2 = 0.196\,71$ e+1, $n = 64$, and a right-hand side contaminated by additive zero mean random noise at a relative noise level of 5%.

	L-curve	FP	FP	DP
λ	$0.857\,82 \times 10^{-7}$	$0.469\,21 \times 10^{-5}$	$0.756\,81 \times 10^{-2}$	$0.161\,55 \times 10^{-1}$
$\|f_\lambda\|_2$	$0.657\,39 \times 10^{2}$	$0.654\,35 \times 10^{2}$	$0.193\,63 \times 10^{1}$	$0.176\,16 \times 10^{1}$
$\|r_\lambda\|_2$	$0.306\,22 \times 10^{-3}$	$0.306\,93 \times 10^{-3}$	$0.939\,40 \times 10^{-2}$	$0.133\,16 \times 10^{-1}$

3. Improvements to the fixed-point algorithm

Having understood the convexity properties of the L-curve, we now clearly see that there may exist several convex local corners, a situation in which both LC and FP tend to fail. An example that illustrates this aspect well is the test problem heat from the regularization tools [10]. A particularly interesting property concerning heat (with a noisy right-hand side) is that its L-curve often displays two convex corners and the function ϕ_1 has two fixed-points that minimize Ψ_1. The problem here is that LC delivers a Tikhonov parameter associated with the sharper L-corner and yields a very undersmoothed solution. A similar property holds for the FP-based solution corresponding to the smaller fixed-point of ϕ_1. For illustration, the residual and solution norms as well as the regularization parameters computed, respectively, by LC, FP and DP, are all displayed in table 1.

Observe from this table that the solutions produced by LC and FP, respectively, associated with the sharper L-corner (the parameters of which are displayed in table 1, columns 2–3, see also figure 4), really yield very undersmoothed solutions; this does not happen with the FP-based solution associated with the largest minimizer of Ψ_1 (as displayed in table 1, column 4) and the DP-based solution. The graphs of the L-curve and ϕ_1 are shown in figure 4.

The conclusion that can be drawn from the results of the test problem heat, which we expect to be valid for other problems, is that if ϕ_1 has several fixed-points that minimize Ψ_1 and if the FP algorithm starts with a very small initial guess, as suggested in [1], then there are strong reasons to believe that FP will fail and that the proper parameter in these cases is that associated with the largest minimizer. The purpose of this section is to describe some variants of FP designed to compute such a minimizer. The variants to be introduced rely on the following observations:

(a) The largest convex fixed-point of ϕ_1, when it exists, does not exceed $\frac{\sqrt{3}}{3}\gamma_p$ (see theorem 2).

(b) The function ϕ_1 is strictly increasing and so is its inverse ϕ_1^{-1} (see (1.10)).

3.1. Variants of the FP algorithm

We shall introduce two variants of the FP algorithm. The first variant claims that the largest fixed-point that minimizes Ψ_1 can always be computed as far as the FP algorithm is judiciously initialized. To make this statement precise, note that because of observation (a), it is reasonable to expect $\phi_1(\lambda_0) < \lambda_0$ for $\lambda_0 \approx \frac{\sqrt{3}}{3}\gamma_p$. When this is the case, $\lambda_{k+1} = \phi_1(\lambda_k), k \geqslant 0$, is a decreasing sequence, as ϕ_1 increases with λ, which always converges either to a fixed-point located to the left of λ_0 when $\delta_0 \neq 0$, or to zero when $\delta_0 = 0$ and ϕ_1 has no nonzero fixed-point on the interval $(0, \lambda_0)$. Although the latter case is very difficult to happen in the context of discrete ill-posed problems, in case FP converges to zero we shall say that FP diverged.

Thus, assuming that $\lambda_0 \approx \sqrt{3}\gamma_p/3$ satisfies $\phi_1(\lambda_0) < \lambda_0$, the first variant starts by setting $\mu = 1$ as a default value, and proceeds by computing subsequent iterates until convergence is reached or until divergence is detected. When convergence is reached, a fixed-point λ^* is computed and a test for convexity of the L-curve at λ^* is made. When divergence is detected or when convergence is reached and the convexity test is not satisfied, the parameter μ is adjusted and the iterations restart.

This variant of the FP algorithm will be denoted by FPJS (which stands for the fixed-point algorithm with judicious starting value). A more or less detailed description of FPJS is as follows:

Fixed-point algorithm with judicious starting value (FPJS)
Input: γ_p, tol, ϵ

1. Set $\mu = 1, k = 0, \lambda_0 \approx \sqrt{3}\gamma_p/3$ such that $\phi_\mu(\lambda_0) < \lambda_0$
2. Compute $s_0 = \phi_\mu(\lambda_0)/\lambda_0$.
3. **while** $(|s_k - 1| > tol \ \& \ \lambda_k > \epsilon)$ **do**
   $\lambda_{k+1} \leftarrow \phi_\mu(\lambda_k)$, $s_{k+1} \leftarrow \lambda_{k+1}/\lambda_k$
   $k \leftarrow k + 1$
   end while
4. **if** $(\lambda_k > \epsilon \ \& \ \phi'_\mu(\lambda_k) < 1/\mu)$ **do**
   $\lambda^* = \lambda_k$,
   elseif $(\lambda_k > \epsilon \ \& \ \phi'_\mu(\lambda_k) = 1/\mu)$ **do**
   Set $\lambda_0 = 0.9\lambda_k, k = 0$, and go to step 2
   else do
   Find k^* such that $s_{k^*} = \min s_k$.
   Select $\mu < 1$, set $\lambda_0 = \lambda_{k^*}, k = 0$, and go to step 2
   end if

Although the choice of $\mu < 1$ at step 4 is rarely required when solving discrete ill-posed problems, for completeness we have to consider it. Indeed, this choice is by no means unique and can be made in several ways. Our suggestion is to follow the procedure in [1], or some criterion that takes into account the convexity results of the previous section the user finds appropriate.

In order to describe the second variant of FP, note that while for $\breve{\lambda} > \gamma_p$ the function ϕ_1 satisfies $\phi_1(\breve{\lambda}) > \breve{\lambda}$, for the inverse ϕ_1^{-1} we have $\phi_1^{-1}(\breve{\lambda}) < \breve{\lambda}$ (see observation (b) and

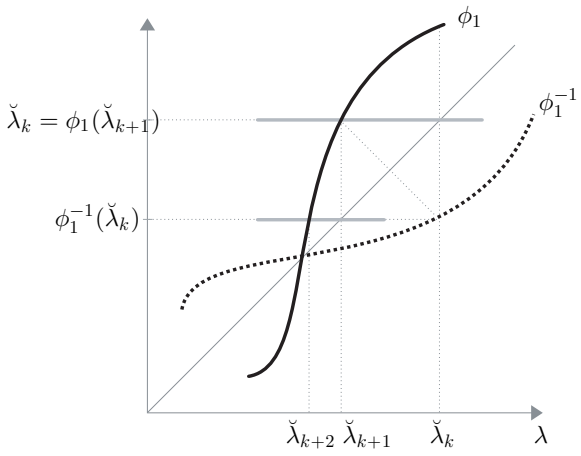

Figure 5. Graphs of ϕ_1 and ϕ_1^{-1}, and two steps of inverse sequence (3.1).

figure 5). Now consider the sequence

$$\breve{\lambda}_{k+1} = \phi_1^{-1}(\breve{\lambda}_k), \qquad k = 0, 1, 2, \ldots \tag{3.1}$$

and call it the 'inverse sequence'. Then, due to observation (b), it follows that the sequence (3.1) is well defined and $\breve{\lambda}_{k+1}$ is the unique solution of the nonlinear equation

$$\vartheta_k(\lambda) \doteq \phi_1(\lambda) - \breve{\lambda}_k = 0. \tag{3.2}$$

Yet, if $\phi_1(\breve{\lambda}_k) > \breve{\lambda}_k$, then $\breve{\lambda}_{k+1}$ is located to the left of $\breve{\lambda}_k$ (see figure 5 again). An immediate generalization of this result is that if ϕ_1 is guaranteed to have fixed-points, then the inverse sequence converges to a fixed-point of ϕ_1 that is to the left of $\breve{\lambda}_0$ if $\phi_1(\breve{\lambda}_0) > \breve{\lambda}_0$, or to a fixed-point of ϕ_1 that is to the right of $\breve{\lambda}_0$ if $\phi_1(\breve{\lambda}_0) < \breve{\lambda}_0$. Therefore, if ϕ_1 has at least one fixed-point and the inverse sequence starts with $\breve{\lambda}_0 > \gamma_n$, then $\lim_{k\to\infty} \breve{\lambda}_k = \lambda_*$ where λ_* is the largest fixed-point of ϕ_1.

With regard to the computation of $\breve{\lambda}_{k+1}$, it can be done in several ways. If we choose a variant of the secant method, for instance, with γ satisfying $\vartheta_k(\gamma) < 0$ and $\breve{\lambda}_k$ as mentioned before (which ensures the root $\breve{\lambda}_{k+1} \in [\gamma, \breve{\lambda}_k]$), this computation can be done as follows:

Inverse sequence via the regula falsi method
Input: tol, γ such that $\vartheta_k(\gamma) < 0$, and $\breve{\lambda}_k$ such that $\phi_1(\breve{\lambda}_k) > \breve{\lambda}_k$

1. Set $u = \breve{\lambda}_k$, $j \leftarrow 0$
2. **while** $|\vartheta_k(\gamma)| > tol$ **do**
   $a = \frac{\phi_1(\gamma)-\phi_1(u)}{\gamma-u}$
   $d_j = \gamma - \frac{\phi_1(\gamma)-\breve{\lambda}_k}{a}$
   if $\vartheta_k(d_j) \leqslant 0$ **do**
   $\gamma \leftarrow d_j$, $j \leftarrow j+1$
   else do
   $u \leftarrow d_j$, $j \leftarrow j+1$
   end if

The second variant, which we denote by FPIS, combines the inverse sequence (3.1) and FPJS. More precisely, we propose to determine the largest concave fixed-point via the inverse

sequence, and then proceed with FPJS in order to compute the sought convex fixed-point. By convex (resp. concave) fixed-point we mean a fixed-point of ϕ_1 at which the L-curve is locally convex (resp. concave). FPIS can be roughly described as follows:

Fixed-point algorithm with inverse sequence as preliminary step (FPIS)
Input: γ_p, tol, ϵ
1. Set $\check{\lambda}_k \approx \gamma_p$ and apply inverse iteration to determine λ_* such that $\phi_1'(\lambda_*) > 1$.
2. Set $\lambda_0 = 0.9\lambda_*$ and resort to FPJS

Note that because every iteration step of the inverse sequence requires solving a nonlinear problem, the inverse sequence should be used not to compute the largest concave fixed-point to high precision, but just as a mean to approximately locate it. Note also that in cases where ϕ_1 has a unique convex fixed-point, all versions of FP (i.e., the original one and corresponding variants) are able to capture it; the only difference is the type of sequence used in its computation: while the original version uses an increasing sequence, the variants use a decreasing one.

We end the section with some observations which should be taken into account in order to fully exploit the potentiality of the FP algorithm.

(O1) Input parameters tol and ϵ play the role of convergence test parameters and are to be fixed by the user. As for the input parameter γ_p, it must be estimated efficiently when the G(SVD) is not available, and a way to do this is by using the Lanczos method applied to $[A^T L^T]^T$.

(O2) In some problems the condition $\phi_1(\lambda_0) < \lambda_0$ for λ_0 near $\sqrt{3}\gamma_p/3$, as required at step 1 of FPJS, may not be satisfied. Indeed, this can happen either because ϕ_1 has no fixed-point (see the analysis of the test problem helio in [1]) or because the condition $\phi_1(\lambda) < \lambda$ is satisfied only near the smallest singular value. In order to handle this difficulty two approaches are suggested. The first one is to apply FPIS as described above. We believe this is the most efficient way to capture the largest convex fixed-point, but extra work is needed. However, numerical experiments show that the extra work spent with FPIS is not substantial provided that the chosen zero finder 'works' at low precision. A numerical example that illustrates the approach and the work spent when applied to the test problem Phillips from [10] is displayed in figure 6. In this case, we consider data corrupted by additive zero mean random noise scaled so that the relative noise level is 10%, and we use regula falsi as zero finder with a convergence test parameter 0.1; inverse iterations terminated as soon as the relative change of consecutive iterates was 0.01. The amount of work required for the computation of the sought largest convex-fixed point via FPIS comprises 5 inverse iterations at a cost of 13 evaluations of ϕ_1 plus 10 FJPS iterations (i.e., plus 10 evaluations of ϕ_1). This test problem is representative of the convergence behavior of FPIS we have observed with other test problems and for several noise levels. Despite this, we do not have a precise recipe which indicates when and under which circumstance one must start with FPIS.

The second one, is to evaluate ϕ_1 at a few values of λ to the left of λ_0, say at $\lambda_1, \ldots, \lambda_q$, in order to know whether the function $\phi_1(\lambda) - \lambda$ changes sign along these values, and in case the difficulty persists, our recommendation is resorting to the original version of the FP algorithm. A similar observation applies for FPIS.

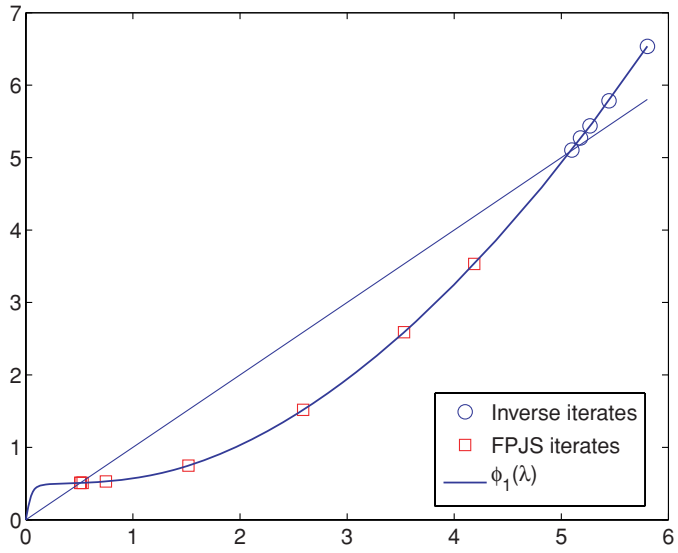

Figure 6. Computation of the largest convex fixed-point of ϕ_1 via FPIS for the test problem Phillips from [10].

4. Numerical results

To evaluate the effectiveness of one of the proposed variants, we have solved the test problem heat with a noisy right-hand side, $\widetilde{g} = g + e$, where e is a zero mean random vector. This test problem was chosen because its L-curve very often exhibits more than one convex corner (see figure 4), in which case both LC and FP (original version) tend to fail. Our intention is thus to illustrate the performance of the FP variants on a problem with difficulties not encountered in the test problems addressed in [1], where the L-curve (resp. function ϕ_1) is shown to have a unique convex corner (resp. a unique convex fixed-point), and where a comparison with LC and GCV is made.

We report average values and standard deviations of 100 realizations with distinct right-hand sides such that $\|\widetilde{g} - g\|_2/\|g\|_2 = 0.01, 0.05$ and $N = 256$. For comparison, we also report results obtained by L-curve, GCV, DP and OPT. OPT stands for a method that calculates the optimal regularization parameter via exhaustive search (which is always possible since the exact solution is known). It is instructive to recall that DP can be considered in two distinct circumstances: one in which DP is almost optimal in the sense that the solution error norm, $\|f^{\text{exact}} - f_\lambda\|_2$, is almost minimized (which is known to occur when the error norm $\|e\|_2$ is provided as an input parameter [4, 17]), and another one in which only an estimate of the error norm is available. Thus, in order to evaluate the effectiveness of FP against DP, two cases are considered. In the first case we provide the error norm as input data, and in the second case we provide an error norm estimate given by $1.05\|e\|_2$. On the other hand, because LC failed constructing reasonable solutions several times, average value computation for LC was done using successful runs only: an LC-based solution was considered successful when the corresponding error did not exceed 1.5 times the maximum error obtained by DP. A similar comment applies for GCV. All computations were carried out in MATLAB using the regularization toolbox described in [10]. As in [1], we use a convergence test parameter defined by the relative change in λ_k: $|\lambda_{k+1} - \lambda_k|/\lambda_k = |s_k - 1| < 10^{-4}$ (i.e., we use $tol = 10^{-4}$). The other convergence test parameter used in the simulation was $\epsilon = 10^{-8}$.

Table 2. Numerical results for the test problem heat. $Iter_{\max} = 12$, $Iter_{\min} = 11$.

	Noise level 1%					
	FPJS	L-curve	GCV	DP	DP$^{\#}$	OPT
SR	100%	24%	59 %	100%	100%	100%
$\overline{\mathrm{E}}$	$0.117\,02 \times 10^{0}$	$0.118\,16 \times 10^{0}$	$0.110\,47 \times 10^{0}$	$0.100\,43 \times 10^{0}$	$0.112\,61 \times 10^{0}$	$0.966\,52 \times 10^{-1}$
$E_{\max}$	$0.126\,75 \times 10^{0}$	$0.126\,88 \times 10^{0}$	$0.125\,24 \times 10^{0}$	$0.127\,10 \times 10^{0}$	$0.137\,93 \times 10^{0}$	$0.124\,52 \times 10^{0}$
$E_{\min}$	$0.965\,33 \times 10^{-1}$	$0.102\,08 \times 10^{0}$	$0.845\,26 \times 10^{-1}$	$0.708\,43 \times 10^{-1}$	$0.820\,50 \times 10^{-1}$	$0.656\,07 \times 10^{-1}$
$\overline{\lambda}$	$0.180\,24 \times 10^{-2}$	$0.174\,88 \times 10^{-2}$	$0.214\,72 \times 10^{-2}$	$0.412\,74 \times 10^{-2}$	$0.522\,52 \times 10^{-2}$	$0.341\,09 \times 10^{-2}$
$\mathrm{STD_E}$	$0.785\,88 \times 10^{-2}$	$0.715\,73 \times 10^{-2}$	$0.107\,58 \times 10^{-1}$	$0.128\,98 \times 10^{-1}$	$0.113\,69 \times 10^{-1}$	$0.130\,23 \times 10^{-1}$
STD_λ	$0.235\,06 \times 10^{-4}$	$0.762\,03 \times 10^{-4}$	$0.153\,54 \times 10^{-3}$	$0.285\,50 \times 10^{-3}$	$0.200\,97 \times 10^{-3}$	$0.342\,75 \times 10^{-3}$

Table 3. Numerical results for the test problem heat. $Iter_{\max} = 14$, $Iter_{\min} = 12$.

	Noise level 5%					
	FPJS	L-curve	GCV	DP	DP$^{\#}$	OPT
SR	100%	66%	72 %	100%	100%	100%
$\overline{\mathrm{E}}$	$0.203\,71 \times 10^{0}$	$0.198\,94 \times 10^{0}$	$0.216\,10 \times 10^{0}$	$0.204\,36 \times 10^{0}$	$0.267\,17 \times 10^{0}$	$0.194\,46 \times 10^{0}$
$E_{\max}$	$0.256\,56 \times 10^{0}$	$0.263\,43 \times 10^{0}$	$0.262\,04 \times 10^{0}$	$0.265\,37 \times 10^{0}$	$0.312\,12 \times 10^{0}$	$0.256\,55 \times 10^{0}$
$E_{\min}$	$0.146\,47 \times 10^{0}$	$0.131\,50 \times 10^{0}$	$0.136\,50 \times 10^{0}$	$0.134\,18 \times 10^{0}$	$0.223\,32 \times 10^{0}$	$0.129\,44 \times 10^{0}$
$\overline{\lambda}$	$0.100\,83 \times 10^{-1}$	$0.739\,12 \times 10^{-2}$	$0.542\,87 \times 10^{-2}$	$0.102\,92 \times 10^{-1}$	$0.171\,41 \times 10^{-1}$	$0.812\,09 \times 10^{-2}$
$\mathrm{STD_E}$	$0.217\,74 \times 10^{-1}$	$0.304\,21 \times 10^{-1}$	$0.267\,78 \times 10^{-1}$	$0.259\,95 \times 10^{-1}$	$0.178\,35 \times 10^{-1}$	$0.262\,25 \times 10^{-1}$
STD_λ	$0.167\,64 \times 10^{-3}$	$0.339\,40 \times 10^{-3}$	$0.503\,76 \times 10^{-3}$	$0.967\,34 \times 10^{-3}$	$0.608\,31 \times 10^{-3}$	$0.919\,10 \times 10^{-3}$

To describe the results we use the following notation:

- SR: successful runs,
- $\overline{\mathrm{E}}$, $\overline{\lambda}$: average values of relative error in f_λ and in Tikhonov parameters, respectively,
- $E_{\max}$, $E_{\min}$: maximum and minimum error, respectively, occurring in all realizations,
- $\mathrm{STD_E}$, STD_λ: standard deviations of computed errors and Tikhonov parameters, respectively.

The results of the experiment using FPJS with an initial guess $\lambda_0 = \sqrt{3}\gamma_p/3$ are shown in tables 2 and 3. Results of DP for the case where we used an error norm estimate instead of the exact error norm are denoted by DP$^{\#}$. From this table, we see that both L-curve and GCV have difficulties computing acceptable solutions, and that if we consider successful runs only, on average FP, L-curve, GCV and DP, all yield solutions with approximately the same quality and close to that yielded by OPT. Further, we see that among the tested methods, the one that estimates more consistently (smallest variance) the regularization parameters is FP, while the one in the opposite direction (largest variance) is DP. This is also illustrated in figure 7. Apart from this, we also see that the error norm in f_λ for DP$^{\#}$ is in agreement with what is known from theory: the error associated with DP-based solutions grows approximately in the same proportion as the estimate for the error norm $\|e\|_2$ does [4, 17]. Also, in order to illustrate how expensive FPJS is, we report the maximum/minimum number of evaluations of ϕ_1 required in the experiment; this is denoted by $Iter_{\max}$, $Iter_{\min}$, respectively. The remaining quantities, namely $E_{\max}$, $E_{\min}$ and, $\mathrm{STD_E}$, do not change very much from a method to another one and no further comments are required.

We end the section with the observation that an implementation of FPIS with regula falsi as zero finder produced solutions with the same precision as that of FPJS, with the difference

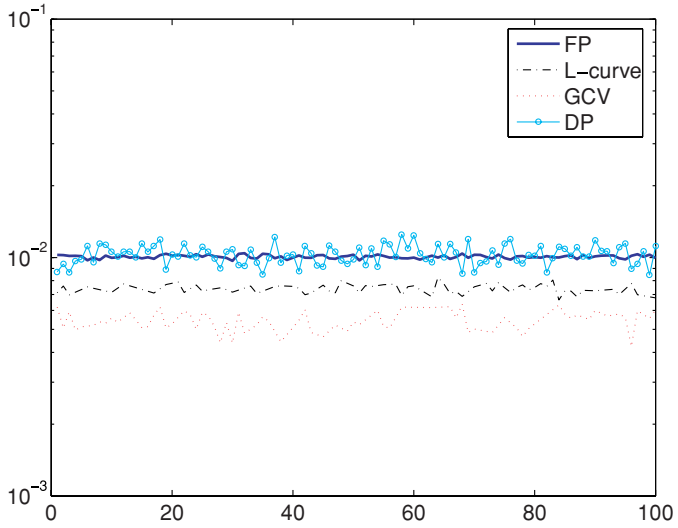

Figure 7. Regularization parameters determined by FP, L-curve, GCV and DP on a logarithmic scale. For L-curve and GCV are considered successful runs only.

that the work spent with the former was about twice the work spent with the latter. This difference can be reduced provided another zero finder is used.

5. Conclusions

Using a model problem with associated L-curve displaying several convex corners, we showed numerically that both the L-curve method (as implemented in [10]) and the FP algorithm (original version) tend to fail. In order to circumvent this difficulty, we investigated the convexity properties of the L-curve in a log–log scale, obtaining results that provide insight into the Tikhonov parameter choice problem and that can be used for improvement of the L-curve method in order to reduce failures. Specifically, new versions of the L-curve method that search for the rightmost *convex* L-corner must be implemented and evaluated numerically. Our main conclusion is that the proper Tikhonov parameter, in cases where the L-curve displays more than one convex L-corner, is the parameter associated with the largest convex fixed-point of ϕ_μ. This gave rise to two variants of the FP algorithm which were evaluated numerically by comparing FP-based solutions with those provided by LC, GCV, DP and a method that gives the optimal regularization parameter. The simulation results not only illustrate that the improved versions of FP can give solutions with essentially the same quality as those provided by well-respected methods such as DP (in its almost optimal version), LC and GCV, but also confirm the excellent performance of FP already shown in [1] where the method is shown to work *successfully* in *all* runs when applied to other problems. This makes the FP algorithm attractive for discrete ill-posed problems. In spite of this, we are aware that further numerical simulation addressing other problems is needed in order to fully assess the performance of FP. This is the subject of future research.

Acknowledgments

The authors are indebted to the referees for their careful reading of this paper and for their constructive criticism that improved both the quality and the presentation of this work.

References

[1] Viloche Bazán F S 2008 Fixed-point iterations in determining the Tikhonov regularization parameter *Inverse Problems* **24** 035001

[2] Belge M, Kilmer M E and Miller E L 2002 Efficient determination of multiple regularization parameters in a generalized L-curve framework *Inverse Problems* **18** 1161–83

[3] Golub G H, Heath M and Wahba G 1979 Generalized cross-validation as a method for choosing a good ridge parameter *Technometrics* **21** 215–22

[4] Groetsch C W 1984 *The Theory of Tikhonov Regularization for Fredholm Equations of the First Kind* (Boston: Pittman)

[5] Hämarik U and Raus T 2006 On the choice of the regularization parameter in ill-posed problems with approximately given noise level of data *J. Inverse Ill-Posed Problems* **14** 251–66

[6] Hämarik U, Palm R and Raus T 2007 Use of extrapolation in regularization methods *J. Inverse Ill-Posed Problems* **15** 277–94

[7] Hansen P C 2001 The L-curve and its use in the numerical treatment of inverse problems *Computational Inverse Problems in Electrocardiology* ed P Johnston (Southampton: WIT Press) pp 119–42 (invited chapter)

[8] Hansen P C and O'Leary D P 1993 The use of the L-curve in the regularization of discrete ill-posed problems *SIAM J. Sci. Comput.* **14** 1487–503

[9] Hansen P C 1998 *Rank-deficient and Discrete Ill-Posed Problems* (Philadelphia: SIAM)

[10] Hansen P C 1994 Regularization tools: a MATLAB package for analysis and solution of discrete ill-posed problems *Numer. Algorithms* **6** 1–35

[11] Johnston P R and Gulrajani R M 2002 An analysis of the zero-crossing method for choosing regularization parameter *SIAM J. Sci. Comput.* **24** 428–42

[12] Krawczy-Stando D and Rudnicki M 2007 Regularization parameter selection in discrete ill-posed problems—the use of the U-curve *Int. J. Appl. Math. Comput. Sci.* **17** 157–64

[13] Kilmer M E and O'Leary D P 2001 Choosing regularization parameters in iterative methods for ill-posed problems *SIAM J. Matrix Anal. Appl.* **22** 1204–21

[14] Morozov V A 1984 *Regularization Methods for Solving Incorrectly Posed Problems* (New York: Springer)

[15] Regińska T 1996 A regularization parameter in discrete ill-posed problems *SIAM J. Sci. Comput.* **3** 740–9

[16] Rust B W and O'Leary D P 2008 Residual periodograms for choosing regularization parameters for ill-posed problems *Inverse Problems* **24** 034005

[17] Vogel C R 2002 *Computational Methods for Inverse Problems, Frontiers in Applied Mathematics* (Philadelphia: SIAM)

[18] Tikhonov A N 1963 Solution of incorrectly formulated problems and the regularization method *Sov. Math. Dokl.* **4** 1035–8

[19] Zibetti M V W, Bazán F S V and Mayer J 2008 Determining the regularization parameters for super-resolution problems *Signal Process.* **88** 2890–901